NJC

Accepted Manuscript

This is an *Accepted Manuscript*, which has been through the Royal Society of Chemistry peer review process and has been accepted for publication.

Accepted Manuscripts are published online shortly after acceptance, before technical editing, formatting and proof reading. Using this free service, authors can make their results available to the community, in citable form, before we publish the edited article. We will replace this *Accepted Manuscript* with the edited and formatted *Advance Article* as soon as it is available.

You can find more information about *Accepted Manuscripts* in the Information for Authors.

Please note that technical editing may introduce minor changes to the text and/or graphics, which may alter content. The journal's standard Terms & Conditions and the Ethical guidelines still apply. In no event shall the Royal Society of Chemistry be held responsible for any errors or omissions in this *Accepted Manuscript* or any consequences arising from the use of any information it contains.

ROYAL SOCIETY OF CHEMISTRY

www.rsc.org/njc

Network-forming polymerization of methacrylamide gelatin and polyacrylamide generates hybrid scaffolds with controlled biocompatibility, porosity and water affinity.

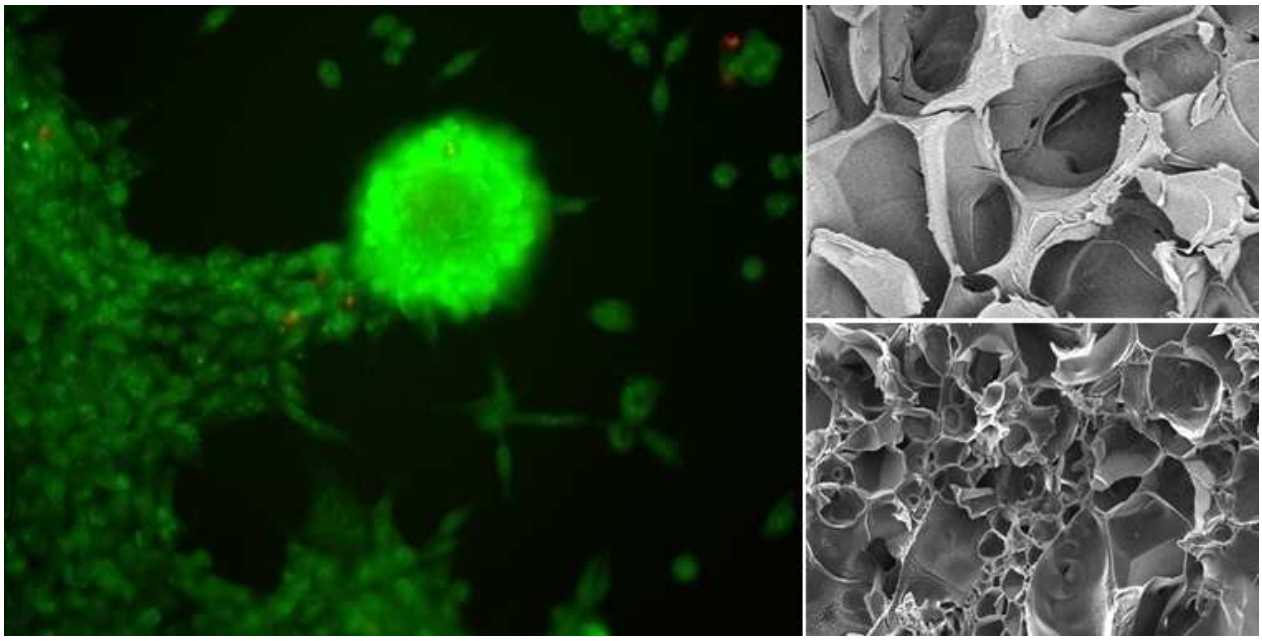

Journal Name

RSCPublishing

ARTICLE

One-pot synthesis of superabsorbent hybrid hydrogels based on methacrylamide gelatin and polyacrylamide. Effortless control of hydrogel properties through composition design.

Cite this: DOI: 10.1039/xoxxooooox

Received ooth January 2012,
Accepted ooth January 2012

DOI: 10.1039/xoxxooooox

www.rsc.org/

Andrada Serafim,[a]† Catalin Tucureanu,[b]† Daniela-Geta Petre,[a] Diana-Maria Dragusin,[c] Aurora Salageanu,[b] Sandra Van Vlierberghe,[c] Peter Dubruel,[c] Izabela-Cristina Stancu[a*]

Biocompatible methacrylamide-modified gelatin (GELMA) hydrogels with tuned characteristics, obtained through network-forming photopolymerization, have recently attracted increasing attention due to their wide range of possible applications such as drug release, tissue regeneration and generation of bioartificial implants. Due to the controlled number of C=C bonds, GELMA may simultaneously act as macromonomer and crosslinker leading through polymerization to hydrogels with rationally designed performances. This study provides effortless one-pot synthesis of hybrid hydrogels based on covalently linked GELMA and polyacrylamide (PAA), using a photo-induced network-forming polymerization. Conventional synthesis of similar hydrogels leads to interpenetrating gelatin and PAA networks, usually involving multistep crosslinking of the components and the use of toxic crosslinkers. Through the described one-pot chemistry the synthetic water superabsorbent PAA with its well-recognized advantages can rationally benefit from the high biocompatibility and cell-adherence of GELMA in a simple covalent way. This work provides a correlation between the composition and the corresponding hydrogel properties (including swelling, pH influence, mechanical behaviour, ability to generate porous scaffolds, enzymatic degradation). The addition of PAA modulated the network density and the water affinity allowing the control of elasticity and degradability. Supplementary crosslinking of the synthetic component provided additional control over the hydrophilicity. The capacity of such hydrogels to generate porous scaffolds was proved; interesting morphologies were developed only by varying the composition. *In vitro* cellular studies indicated that the presence of GELMA conferred controlled cell-affinity properties to the bicomponent hydrogels. Nevertheless, the drug release potential of such hydrogels was preliminary investigated using sodium nafcillin. GELMA-PAA hydrogels may be useful for tissue regeneration due to the effortless synthesis, compositional flexibility and variable properties.

1. Introduction

Hydrogels are hydrophilic polymers with intrinsic three-dimensional (3D) structure extensively studied as biomaterials due to their mechanical, physico-chemical and functional resemblance with the extracellular matrix (ECM). These materials are water insoluble, soft and elastic when hydrated, and represent interesting scaffolds for tissue engineering, cell encapsulation and drug delivery applications. Van Vlierberghe et al. recently reviewed key aspects related to biopolymer-based hydrogels with applications in tissue engineering [1]. Unlike natural hydrogels, synthetic counterparts present as main advantage the possibility to control their composition, polymerization, degradation, mechanical behaviour and even biocompatibility. Accordingly, synthetic hydrogels can be, from a chemical point of view, better defined and developed with a panel of selected properties adapted to provide the best outcome with respect to key characteristics of the ECM [2]. Furthermore, it is recognized that synthetic hydrogels reduce the variability between *in vitro* studies and decrease the potential immunorejection [2]. However, their lack of biological cues and cell recognition features justify the need to further combine these materials with natural components to enable their biomedical application. Various routes to control and improve the *in vitro* and *in vivo* performance of natural and synthetic hydrogels have already been developed and resulted in covalently modified hydrogels [3, 4], multicomponent hydrogels such as semi- or

interpenetrating polymer networks [4-9], or a more complex combination thereof. Providing natural polymers such as peptides, proteins and polysaccharides with a synthetic polymerizable moiety e.g. (meth)acrylamide is a smart chemical strategy to further generate hydrogels through controlled polymerization of the C=C bond, similarly to synthetic vinyl-based monomers. It becomes a common procedure nowadays to modify a natural polymer with (meth)acrylamide side chains in order to photopolymerize it in a next stage to produce polymer networks. The characteristics of the so-generated hydrogels may be tuned through the manipulation of the (meth)acrylation degree and the polymerization feed ratio. Hydrogels based on methacrylated gelatin [1, 4, 10-21], tropoelastin [22], hyaluronic acid [10, 21], dextran [23], gellan gum [12], chitosan [24] and sericin [25] are only few examples. These (photo)crosslinked functional mimetic gels present innate biological features of the corresponding natural polymers and open a wide range of applications for tissue engineering. The application of such synthetic polymerization pathways overcomes some drawbacks of natural polymers (e.g. the photopolymerization allows polymer crosslinking without addition of toxic crosslinkers such as glutaraldehyde and without a heating step which could potentially damage temperature-sensitive molecules). Even so, the natural hydrogels obtained in such a manner are still associated with modest mechanical properties, sometimes too fast biodegradation, and accordingly, limited biomedical applications. Therefore, in this work we intend to go one step further by using a synthetic polymerization path to generate novel hybrid hydrogels based on covalently combined natural and synthetic components.

GELMA is a bioactive macromolecule acting both as macromonomer and crosslinking agent when exposed to polymerization conditions (i.e. redox initiation, UV initiation). It is obtained through the modification of primary amines of (hydroxyl)lysine residues from the gelatin chain. Through photopolymerization, GELMA generates networks with tunable properties intensively explored for various applications including tissue regeneration, bioartificial organs or drug release [1, 11, 12, 14-18, 20-22, 26, 27]. GELMA hydrogels present most of the advantages of gelatin, one major benefit being the similarity with ECM components, this leading to the ability to stimulate the cellular response or the enzymatic degradability by metalloproteinase. However, one drawback of these gelatin-based hydrogels remains their mechanical weakness. While GELMA is an appealing polymerizable collagenous derivative, with all biocompatibility-related attributes, acryl synthetic monomers remain a critical component of many biomedical products addressing continuously changing marketplaces.

The aim of the present work is to develop a one-pot synthesis method in order to synergistically combine the well-known innate biological properties of gelatin with the practical advantages of a synthetic hydrophilic biocompatible polymer, polyacrylamide (PAA). In this respect network-forming free radical photopolymerization of C=C bonds from GELMA and acrylamide was used. PAA is a conventional inert synthetic hydrogel, recently considered appealing for the development of multicomponent superabsorbant and eventually porous scaffolds for various tissue regeneration or drug release uses [6, 9, 28]. Its main applications as biomaterial are revised in [29]. PAA can be prepared through the free radical polymerization of the corresponding monomer, acrylamide, in the presence of the crosslinker N,N'-methylenebis(acrylamide). This study presents how GELMA-PAA hybrid hydrogels with covalently linked components and tunable water affinity, degradability and mechanical behaviour can be prepared through a one-pot effortless network-forming polymerization, by simple modification of the composition of the polymerization mixture. GELMA acts as crosslinking agent and also as a co-macromonomer in the polymerization of acrylamide. The network density of the so-obtained bicomponent hydrogel is modified through the addition of PAA when compared to individual GELMA hydrogels. Properties such as water affinity and elasticity are investigated. Conventional synthesis of similar hydrogels leads to interpenetrating gelatin and PAA networks, and usually involves multistep crosslinking of the components and the use of toxic crosslinkers. Through the one-pot chemistry described in this work, the synthetic water superabsorbent PAA with its well-recognized advantages can rationally benefit from the high biocompatibility and cell-adherence of GELMA, in a simple, covalent way. Additional crosslinking of PAA with a synthetic crosslinker further improves the mechanical behaviour. The ability of such materials to generate porous scaffolds with various morphologies is also emphasized. In addition, this preliminary work investigates the biocompatibility and the drug release potential of GELMA-PAA bicomponent hydrogels as well as the ability to promote cell adherence. Due to the dual nature, synthetic (PAA component) versus natural (GELMA component), and to the simplicity of the polymerization reactions under mild conditions providing control over the properties of the resulting materials, the GELMA-PAA hydrogels developed in this work may be suitable for a wide range of biomedical applications.

2. Experimental

2.1. Materials. Gelatin (type B), isolated from bovine skin by an alkaline process, was supplied by Sigma-Aldrich (Steinheim, Germany). In this study, gelatin methacrylamide (GELMA) was prepared and further used to synthesize bicomponent hydrogels. GELMA was obtained via methacrylation of primary amino groups from gelatin, through a reaction with methacrylic anhydride (MA), as previously described [4]. MA (94%) was purchased from Sigma-Aldrich and used as received. The degree of substitution (DS) of GELMA represents the ratio of so-formed methacrylamide side groups with respect to initial amino groups from gelatin and it was determined by proton nuclear magnetic resonance (^{1}H-NMR) spectroscopy [4]. GELMA was further used as a 10% w/v solution in double distilled water (ddw).

1-[4-(2-Hydroxyethoxy)-phenyl]-2-hydroxy-2-methyl-1-propane-1-one] (Irgacure 2959), acrylamide (AA) (for electrophoresis, ≥99%) and N,N'-methylenebis(acrylamide) (MBA) were purchased from Sigma-Aldrich and used as such.

Bicinchoninic Acid (BCA) kit for protein determination was purchased from Sigma–Aldrich; the kit contains reagent A: BCA solution and reagent B: 4% (w/v) $CuSO_4.5H_2O$ solution.

Collagenase Type I of Clostridium histolyticum with a collagen activity ≥ 125 units per mg (collagen digestion units) was from Sigma Chemical Co. All the salts necessary to prepare phosphate buffer saline (PBS) and ethylene diamine tetraacetic acid (tetra sodium salt tetrahydrate) (EDTA) were supplied by Sigma-Aldrich. Sodium azide (99%) was purchased from Avocado Research Chemicals Ltd. Nafcillin sodium salt monohydrate was supplied from Sigma.

2.2. One-pot synthesis of GELMA-PAA hydrogels through network-forming photopolymerization. Bicomponent hydrogels were obtained through a one step network-forming polymerization reaction of C=C bonds from AA and GELMA. Polymerization mixtures containing GELMA and synthetic monomer with(out) synthetic crosslinking agent were prepared at 40°C, varying the amount of components based on the ratio between their C=C groups in the interval AA/GELMA from 25/1 to 1000/1. The synthesis method is simple, consisting in a one step photopolymerization of the C=C bonds from the

reaction mixture. The compositions were selected in order to investigate: (1) the effect of different amounts of gelatin and synthetic polymer and (2) the effect of the crosslinking with MBA on the selected properties of the scaffolds developed.

The synthesis procedure was adapted from a previously reported study [4]. In brief, aqueous GELMA solution (10% wt) was prepared and the corresponding volume of AA solution was added under vigorous stirring, at 40°C. The total solid content was maintained at 15%. Then, the corresponding amount of photoinitiator Irgacure 2959 (aqueous solution with a concentration of 2 mol% with respect to the methacrylamide side groups in GELMA and 0.1 mol% with respect to the C=C groups from AA) was added. After subsequent homogenization, the polymerization mixtures were degassed using an ultrasound bath and then were poured in Petri dishes. All the polymerization reactions were performed for 30 minutes, using a multiband transilluminator ECX-F26, at a wavelength of 312 nm. The obtained GELMA–PAA hydrogels were further denoted P1-P4, according to an increasing AA concentration going from 50/1 to 1000/1 (table 1).

In addition to P1-P4, a second series of GELMA-PAA hydrogels was synthesized using the same procedure described above, after supplementing the reaction medium with a synthetic crosslinking agent, MBA. Briefly, GELMA and AA-MBA aqueous solutions were prepared through dissolution of the reagents in ddw using 1% (molar) MBA with respect to AA. Four bicomponent mixtures were obtained, with the ratio of C=C groups from AA/GELMA of 25/1, 50/1, 100/1, and 1000/1 (table 1). Then, the corresponding amount of initiator was added (aqueous solution with a concentration of 2 mol% with respect to the methacrylamide side groups in GELMA and 0.1 mol% with respect to the C=C groups from both AA as well as MBA). The polymerization was performed for 60 minutes, using a transilluminator ECX-F26, at a wavelength of 312 nm. The corresponding hydrogels were further named T1-T4. The synthetic crosslinker was used in order to influence the network properties even more. Control GELMA and PAA hydrogels (denoted T0 and T0') were prepared using similar synthesis methods.

The resulting materials were submitted to gel fraction analysis in order to estimate the efficiency of the network-forming polymerization. Purification with distilled water was extensively performed prior to other characterization assays.

2.3. Characterization

2.3.1. Efficiency of the network-forming polymerization. The efficiency of the polymerization with respect to the network formation was investigated by gel fraction analysis in ddw and in co-solvent ethanol-ddw (40% ethanol). In a first step, the polymerization products were dried completely at 40°C. The total weight (sol+gel), w_0, was measured. Then, the samples were immersed in ddw, at 40°C, for 72 hours. The remaining gels were completely dried, at 40°C, and their masses, $w_{g,ddw}$, were recorded. Gel fraction (GF_{ddw}%) was estimated using the equation below:

$$GF_{ddw},\% = \frac{w_{g,ddw}}{w_0} \times 100 \quad (1)$$

In a second step, the dried bicomponent hydrogels (of dried mass $w_{0'}$) were incubated in the co-solvent system, for 6 days, at 40°C, and gel fraction (GF_{Eth}%) was calculated again, using the equation (2):

$$GF_{Eth},\% = \frac{w_{g,Eth}}{w_{0'}} \times 100 \quad (2)$$

where $w_{g,Eth}$ is the weight of the dry gel removed from the co-solvent system. The experiment was performed in triplicate.

2.3.2. Fourier-Transform Infrared Spectrometry (FT-IR). GELMA-PAA hydrogels were characterized using a JASCO 4200 spectrometer equipped with a Specac Golden Gate attenuated total reflectance (ATR) device in the 4000–600 cm^{-1} wavenumber region. The recorded spectra were compared with the spectra of the control hydrogels, in order to identify the presence of the specific vibrations of PAA and GELMA in the bicomponent systems.

2.3.3. Determination of swelling ability

The swelling behaviour of the bicomponent hydrogels was investigated in ddw, at 37°C, using the conventional gravimetric method. Briefly, the swelling ratio (*SR*) was calculated at predefined time intervals, using the following equation:

$$SR,\% = \frac{w_t - w_0}{w_0} \times 100 \quad (3)$$

where w_t is the weight of the swollen hydrogel at time t and w_0 is the initial weight of the dry hydrogel before incubation in ddw. The samples were weighed after the excess of water was removed with filter paper. The maximum swelling degree (MSD) represents the maximum value obtained after equilibrium was reached. The equilibrium water content (*EWC*) was calculated using the following equation:

$$EWC,\% = \frac{w_{max} - w_0}{w_{max}} \times 100 \quad (4)$$

where w_{max} is the maximum weight of the swollen gel sample after equilibrium was reached and w_0 is the initial weight of dry gel samples submitted to swelling.

From a kinetic point of view, swelling kinetics were determined using equation (5):

$$f = kt^n \quad (5)$$

where f represents the fractional water uptake, k is a constant specific to the tested hydrogel, t is the swelling time and n is a number indicating whether relaxation or diffusion controls the swelling process. f is calculated as w_t/EWC, where w_t is the water content of the hydrogel at time t. Equation (5) is used to determine the nature of the water diffusion into hydrogels and it is only valid for a fractional water uptake of 0.6 [6].

2.3.4. Mechanical properties.

The mechanical behaviour of the hydrogels swollen at equilibrium in ddw at 40°C was studied using the Brookfield CT3 texture analyzer at room temperature. Cylindrical samples with the diameter of 10 mm and a thickness of 5 mm were fixed on a base plate and uniaxially compressed by the upper plate connected to a 4500 grams cell. The test speed was set at 0.5 mm/s. A stress versus strain graph was plotted. The compression modulus was calculated from the slope of the linear part of the compression curve, at 5% strain.

2.3.5. Morphological examination using scanning electron microscopy.

The surface morphology of GELMA-PAA hydrogels and their porous structure were investigated through Scanning Electron Microscopy (SEM), using a QUANTA INSPECT F SEM device equipped with a field emission gun (FEG) with 1.2 nm resolution and with an X-ray energy dispersive spectrometer (EDS).
Longitudinal sections and cross-sections were obtained from water swollen hydrogel cylinders, using a sharp blade, and then dried.
To obtain porous scaffolds, T1-T4 hydrogels and the control samples T0 and T0' were water-swollen, frozen at -80°C and then freeze-dried (Martin Christ freeze-dryer). Cross-sections were obtained using a sharp blade to reveal the internal porosity. Hydrogels were gold-coated prior to analysis.

2.3.6. *In vitro* degradation study

Equilibrium water content – study of pH influence. The stability of samples immersed in three different buffer solutions with pH values of 3, 7.4 and 11, respectively, was also determined. Dried hydrogel samples were placed in each test solution and the swelling ratio was estimated at predetermined time intervals. As described in the experiment above, the blot and weight method was used. Briefly, each sample was immersed in the corresponding buffer solution and weighed at pre-established time intervals after the excess surface liquid was wiped off with filter paper. The swelling ratio of each sample was calculated using equation (3), as described in [6]. Since mass loss was noticed only for the hydrogels immersed in the buffer with pH 11, BCA assay for protein determination was performed to assess whether or not protein was released. The method was already reported in [30]. The BCA working reagent was prepared as 50 parts reagent A + 1 part reagent B. 0.1 x10^{-3} L sample was mixed with 2 x 10^{-3} L working reagent in the UV cells; the aliquot was incubated at 37°C and measured after 30 min at 562 nm. The concentration of the detected protein was calculated from a calibration curve obtained using gelatin solutions with known concentration. The amount of protein released was estimated ($w_{GELMA,BCA}$) and the mass loss (*ML*, *%*) was estimated with respect to the initial mass of the tested hydrogel (w_0):

$$ML = (w_0 - w_{GELMA,BCA})/ w_0 * 100 \quad (6)$$

Enzymatic degradation. The *in vitro* degradation behaviour of hydrogels was studied using a protocol adapted from [4]. Cylindrical freeze-dried samples (Ø 0.8×0.5 cm) were incubated in 0.5 ml Tris-HCl buffer (0.1 M, pH 7.4) in the presence of 0.005% (w/v) NaN_3 and 5 mM $CaCl_2$ at 37°C. After 1 h, 0.5 ml collagenase solution (200 U/ml), dissolved in Tris-HCl buffer was added. At pre-defined time intervals, the degradation was stopped by addition of 0.1 ml EDTA solution (0.25 M) and subsequent cooling of the samples on ice. Next, the samples were washed three times during 10 min with ice-cooled Tris-HCl buffer and three times with double distilled water. The samples were further dried at 40°C to constant mass. The degradation extent (*DR*, *%*) was determined using the following equation:

$$DR = \frac{w_0 - w_t}{w_0} \times 100 \quad (7)$$

where w_t is the dry mass of the polymer remaining after degradation at time t and w_0 is the initial mass of the dry hydrogel.

2.3.7. Drug release profile

To estimate the release capacity of GELMA-PAA hydrogels, nafcillin was selected as a model drug. The scaffolds were loaded with the antibiotic during their development by the addition of the drug solution (10 mg/ml) into the reaction mixtures, before hydrogel formation (0.200 ml nafcillin solution, per sample). Loaded samples were obtained into 24 wells culture plates. Dried cylinders of known weight were immersed into 10 ml PBS (pH 7.4) as release medium. The incubation was performed in plastic vessels, at 37°C, using a Memmert type WNE 14 adjustable-speed shaking water bath with horizontal movement (speed of 150 strokes per minute, stroke 15 mm back/forth movements). 2 ml of the release medium was removed at predefined time intervals and the absorbance was measured on a CINTRA 101 UV-Vis spectrophotometer. Quartz cells with a 1 cm pathway were used. After the measurement, each sample was poured back into the release vessels. A calibration curve was obtained using antibiotic solutions of known concentrations in the interval 0.002 - 0.125 mg/ml.

2.3.8. Cell seeding on hydrogels

Preparation of hydrogels for cell seeding. Polymerization mixtures were sterilized by passing through 0.45um PVDF syringe driven filter units (Millipore) and poured between sterile standard SDS-PAGE glass plates using 1 mm spacers and exposed to UV radiation for 1 hour to allow polymerization. The gels were removed from the casting moulds and extensively washed for 24h in large volumes of sterile, purified water, and subsequently allowed to swell in cell culture medium for another 24h. Disks closely fitting the well diameter of 96-well cell culture plates were punched out of the gels, transferred to Petri dishes and further washed in sterile water for 48h in order to ensure elimination of toxic contaminants remaining after the polymerization. After an additional 24h swelling in cell culture media, gel disks were transferred to flat-bottom 96-well tissue culture plates.

Cell seeding. L-929 cells were detached by trypsin, counted and resuspended in Dulbecco's Modified Eagle Medium (DMEM) (Sigma-Aldrich) supplemented with 10% fetal bovine serum (FBS) (GIBCO) and 100 U/mL penicillin-streptomycin (Lonza). Cells were seeded at 2x10^4 cells/well for 24h or 1x10^4 cells/well for 7 days and incubated at 37°C in a humidified atmosphere with 5% CO_2, in flat-bottom 96-well tissue culture plates.

Cell culture

MTT assay for cellular viability. Cellular viability was measured using an MTT reduction assay (3-[4,5-dimethylthiazol-2-yl]-2,5-diphenyl tetrazolium bromide – Sigma Aldrich). Non-adherent/loosely adherent cells were removed by pipetting and transferred to separate wells for testing. MTT was added to a final concentration of 0.5mg/mL in DMEM and cells were incubated for 4h at 37°C. Cell-culture plates were centrifuged for 10 minutes at 400G in a swing-out rotor on a Sigma 3-16PK centrifuge to pellet non-adherent cells, and media was carefully removed prior to

addition of 150 µl/well of dimethylsulfoxide and incubation for 1h on a rotary shaker for solubilisation of formazan crystals. Aliquots of 100 µl were transferred to a fresh plate and absorbance at 580 nm was measured on a TECAN Infinite M1000 PRO microplate reader. Absorbance values for samples were normalized to those obtained for cells cultured in the same conditions on tissue culture plastic. Statistical significance for difference between groups was assessed using unpaired, two-tailed student T-test in R.

Fluorescence microscopy. Cells grown for 7 days on bicomponent hydrogels were stained with 2µg/mL acridine orange (AO) and 4µg/mL propidium iodide (PI) in PBS and imaged on a Nikon TE2000U microscope using a 5MP cooled CCD camera and a 20x long working distance objective. For each field, separate grayscale images (16bit TIFF) were taken using epifluorescence filter blocks (AO - λEx 455-495nm, λEm 500-545nm; PI - λEx 510-560nm, λEm 590-600nm) and DIC.

3. Results and discussion

One-pot preparation of the hybrid hydrogel scaffolds through network-forming polymerization

Bicomponent hydrogels were prepared in a way similar to the polymerization of AA to form PAA. Accordingly, GELMA and synthetic structural units were covalently assembled into large natural-synthetic structures through the free radical polymerization of C=C groups from the methacrylamide side groups of GELMA and from the acryl groups of AA. Through this approach, hybrid hydrogels of various compositions were prepared, in an attempt to monitorize the efficiency of this method in developing materials with physico-chemical and biological properties that can be tailored for predefined applications.

The network-forming polymerization was photo-initiated by the radicals provided by Irgacure 2959, at 312 nm. Various networks of inert alkane backbones with pendant interconnected gelatin side chains were formed, depending on the feed composition. Their structures are anticipated to be extremely complex since GELMA is multifunctional and it acts both as macromonomer as well as crosslinking agent, simultaneously. We assume an initial homogeneous distribution of the precursor molecules in the reaction mixture, due to physical interactions between the two types of reagents (i.e. hydrogen bonds). Of course, the different feed ratios play an important role in the assembling of the structural units of different origin in the hybrid hydrogels. Accordingly, complex structures are formed and, depending on the amount of gelatin or synthetic component used, the networks may present coexisting GELMA-GELMA domains (a domains in scheme 1), GELMA-AA sequences (b domains in scheme 1), and either PAA richer sequences in P1-P4 (c domains in scheme 1) or crosslinked PAA in T1-T4 (c and d domains in scheme 1). All hydrogels were obtained as crosslinked products containing the water from the reaction mixtures. They typically appear as soft, elastic, transparent hydrogels, with a yellowish colour proportional to the GELMA content (example in inset in scheme 1).

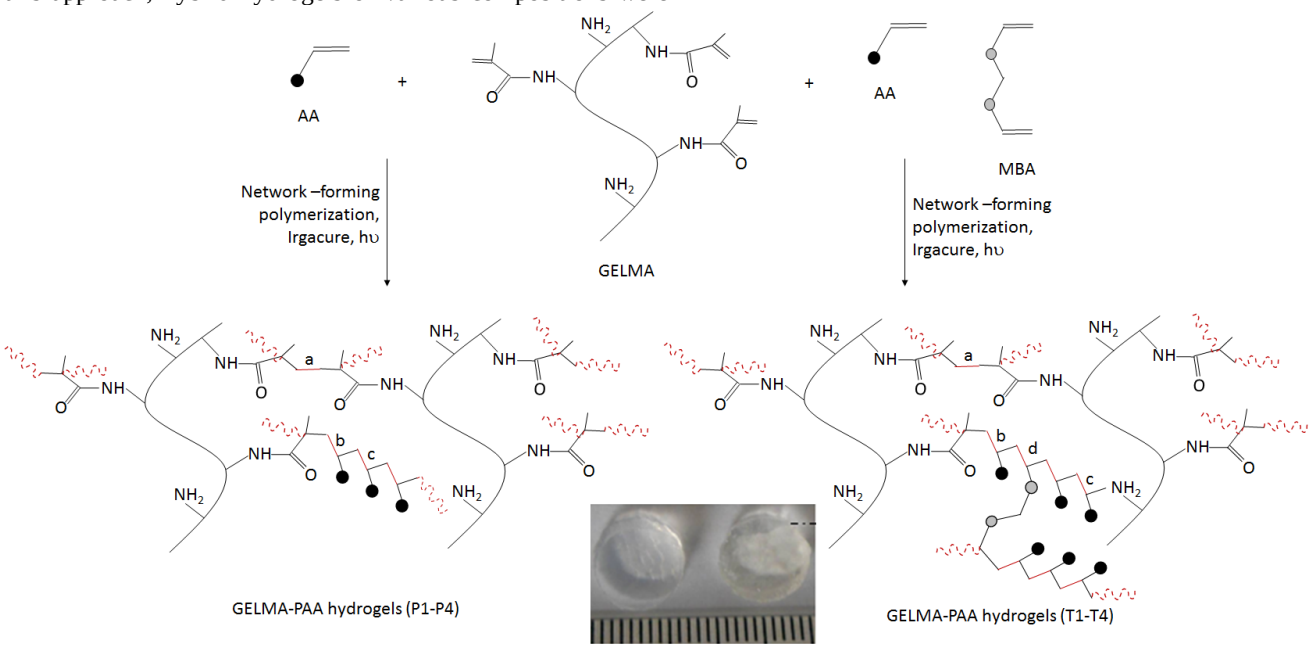

Scheme 1. Schematic simplified view of GELMA-PAA sequences in the bicomponent systems obtained with AA and with AA-MBA. Four types of new C-C bonds are formed during the polymerization of C=C bonds from adjacent: (a) GELMA - GELMA macromolecules; (b) GELMA-AA; (c) AA – AA; (d) AA-MBA. Inset: cylinder hydrogel samples as obtained after the polymerization reaction: left - T4; right - T1.

Gel fraction study

In order to establish the efficiency of network formation through polymerization, all the reaction products were submitted to a gel fraction study. Following polymerization, the hydrogel precursors should ideally form bicomponent networks in a quantitative matter. Such materials are insoluble and therefore, gel fraction analysis allows to quantify, through extraction in appropriate solvents (ddw and ethanol), the potentially remaining soluble fraction. GF values were calculated based on gravimetric measurements and using

equations (1) and (2). The obtained results are presented in table 1. High GF values were obtained, ranging from 92.80 ± 1.76 to 97.95 ± 0.33 in ddw, and from 94.31 ± 0.65 to 98.96 ± 1.21 in the co-solvent system water-ethanol. No significant difference was noticed for GF values when using the synthetic crosslinker, MBA. The data indicate (i) the mass conservation following the chemical treatment and (ii) the insolubility in water of the hydrogels confirming the success of the network formation through one-step free radical polymerization using photoinitiation.

FT-IR analysis

FT-IR analysis confirmed the presence of characteristic functional groups from the two individual polymer components in the synthesized bicomponent systems. GELMA (T0) and PAA (T0') hydrogels were used as control samples. GELMA presents the following specific vibrations: a broad peak at 3283 cm^{-1} (common signal for O-H and N-H stretching), 3077 cm^{-1} (N-H), 2942 cm^{-1} (saturated C-H stretch), 1631 cm^{-1} (amide I) and 1527 cm^{-1} (amide II). PAA shows the following main vibrations: one strong intensity band with two spikes which are visible around 3333 cm^{-1} and 3190 cm^{-1} and undoubtedly associated with the N-H stretching vibrations, while the C-O stretching (amide I) vibration occurs at 1645 $cm^{-1}$and the NH_2 bending (amide II band) can be noticed at 1604 cm^{-1}. The two latter peaks are not well separated, being visible as a strong intensity peak with two spikes. The FT-IR spectra of the synthesized bicomponent systems showed combination of all these vibrations. Decreasing GELMA content with increasing PAA leads to modifications of the specific vibrations, as shown in fig. 1.

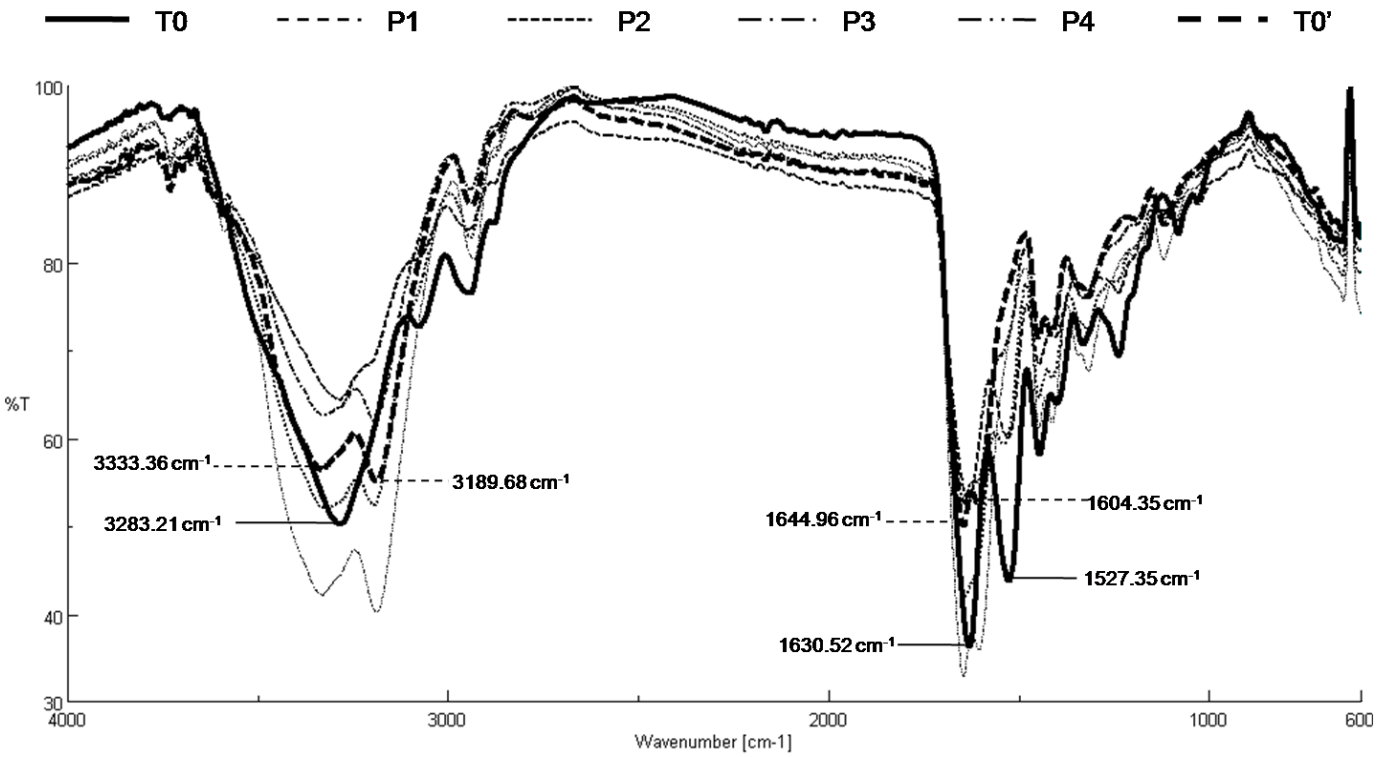

Fig. 1. FT-IR spectra recorded on control samples T0 and T0' and on bicomponent hydrogels P1 – P4 (increasing amount of PAA from P1 to P4 intensifies the specific vibrations characteristic for this component).

Accordingly, increasing PAA in the bicomponent systems from P1 to P4 leads to the following specific spectral changes. The samples P1-P4 present combined broad peaks with two spikes (around 3284 – 3332 cm^{-1}, and 3203 – 3189 cm^{-1}, respectively) characteristic to N-H vibrations from PAA and GELMA overlapping with the O-H stretching vibration from GELMA. The higher PAA content when going from P1 to P4 is associated with a peak shifting to higher wavenumbers. On the other hand, decreasing GELMA while increasing the PAA content from P1 to P4 leads to a strong modification of the amide-characteristic spectral region. Accordingly, increasing PAA in the hybrid hydrogels leads to overlapping and shifting of the amide I and amide II vibrations to higher wavenumbers when compared to GELMA (T0). More specifically, the sample with the lowest PAA content (i.e. P1) has almost the same spectral appearance characteristic to GELMA, with separated peaks for the amide I at 1633 cm^{-1} and the amide II at 1529 cm^{-1}. In addition, the sample with the highest PAA content (i.e. P4) presents only one strong intensity peak with two spikes at 1646 cm^{-1} and 1606 cm^{-1} assigned to the amide I and II from the two components respectively. These values and the shape of the peak are similar to the spectral appearance of PAA (T0').

The FTIR data proved that all the hydrogels present the characteristic signals from GELMA and PAA, providing also the influence of the composition on the spectral appearance.

Effect of composition and crosslinking on the swelling ability

The capacity of hydrogels to absorb water is one of the main characteristics directly impacting on eventual biomedical applications. Swelling ratios of the bicomponent GELMA-PAA hydrogels in ddw, at 37°C were calculated using equation (3) and the obtained data are graphically presented in figure 2. The compositions of the studied hybrids were previously expressed using the ratios between the polymerization-reactive C=C

bonds from AA and GELMA, and the corresponding weight ratios are displayed in table 1.

Hydrogel	*Feed composition ("C=C" ratio) AA/GELMA**	*Feed composition (wt/wt) AA/GELMA**	*Gel Fraction, (%)*	
			ddw	ddw/ethanol solution
P1	50:1	0.56	94.84 ± 0.64	98.96 ± 1.21
P2	100:1	1.12	92.80 ± 1.76	98.16 ± 1.34
P3	500:1	5.6	94.09 ± 1.66	96.69 ± 0.71
P4	1000:1	11.2	96.35 ± 0.67	94.31 ± 0.65
T1	25:1	0.40	93.42 ± 2.13	95.69 ± 1.42
T2	50:1	0.80	97.95 ± 0.33	96.53 ± 0.25
T3	100:1	1.6	96.81 ± 0.89	97.42 ± 0.41
T4	1000:1	16	96.43 ± 0.67	96.85 ± 0.23
T0	0:1`	0/1	98.18 ± 0.54	97.41 ± 0.18
T0'	1:0	1/0	97.98 ± 0.46	98.54 ± 0.14

Table 1. Gel fraction values obtained for GELMA-PAA hydrogels with various composition. (n = 3, mean ± standard deviation)
* total solid content was maintained at 15%, and for samples T1-T4 and T0', MBA was used as 1% molar with respect to AA

Influence of the network density. The swelling behaviour of the bicomponent hydrogels strongly depended on the chemical composition, namely the swelling level was enhanced by increasing acrylamide in the polymerization mixtures or, in other words, by reducing GELMA content. Accordingly, the values of the maximum swelling degree (MSD) increased from P1 to P4. Different swelling abilities were identified as depicted in Figure 2a and Figure 2b and the hydrogel with the highest GELMA content (P1) possessed a MSD value of 1447 ± 11 %. Adding two times more AA in the polymerization mixture resulted in approximately equal GELMA and PAA contribution in the hydrogel P2. Interestingly, the MSD value increased only to 1546 ± 26%. A more important increase of the MSD value occurred for P3 when the AA content was augmented ten times when compared to P1 and five times when compared to P2. The MSD reached in this case 2142 ± 33 %. For the hydrogel P4 with the highest AA content from the series, namely twenty times more AA than in P1 and ten times more AA than in P2, the MSD was 2440 ± 11 %. This behaviour corresponded to a non-linear dependence between the MSD values and the AA/GELMA content. For these materials, GELMA is the crosslinker generating networks with PAA sequences. The hydrogels richer in GELMA would therefore present a denser network and accordingly, a lower swelling capacity.

Influence of hydrophilic components. For the hydrogels prepared with MBA, two main characteristics were observed: (1) as anticipated, the use of MBA reduced the swelling and (2) increasing PAA from T1 to T4 resulted in an augmentation of the water affinity. The use of the synthetic crosslinker MBA significantly increased the network density, thus decreasing the swelling ability of the resulting T1-T4 hydrogels when compared to samples P1-P4 (Figure 2a and 2b). The highest MSD was only 1004 ± 42 % for T4, when compared to the value of 2440 ± 11 % corresponding to the hydrogel P4 prepared using the same ratio AA/GELMA (1000/1 C=C bonds) but without adding MBA. Furthermore, GELMA-PAA hydrogels with increasing PAA content from T1 to T4 presented an increasing swelling trend similarly to the results recorded for samples P1-P4. Similarly, the MSD values were 548 ± 14 % for T1 and 1004 ± 42 % for T4.

On the other hand and very importantly, MSD values determined for the control hydrogels were 405 ± 6 % for GELMA (T0) and 1022 ± 25 % for PAA (T0'). This indicated that when keeping the total solid content constant at a value of 15%, PAA generated a more hydrophilic hydrogel when compared to GELMA.
It is evident that increasing PAA content would enhance the water affinity of the bicomponent hydrogels through the incorporation of more hydrophilic synthetic sequences. These data are very appealing since they provide a way of controlling the water affinity of such hydrogels. This behaviour is even more interesting since our findings differ from other studies, without being contradictory. For example, Mandal [6] and Zaharia [28] reported that increasing the amount of crosslinked PAA results in denser networks with lower water swelling. The materials developed by Mandal [6] and Zaharia [28] are semi-interpenetrating polymer networks (sIPNs) prepared through the polymerization of AA monomer in the presence of a protein (namely silk fibroin). Such procedures result in PAA networks with non-crosslinked fibroin immobilized at molecular level into the hydrogels. Therefore, more crosslinked PAA obtained using a constant MBA/AA ratio results in stronger gels with lower swelling capacity. In our work, GELMA-PAA hydrogels contain covalently combined natural and synthetic sequences forming through polymerization a unique and complex network, as schematically presented in Scheme 1. The balance between the two components is the determining factor increasing or decreasing the swelling. Furthermore, the EWC of all GELMA-PAA hydrogels obtained without MBA was found to be well above 93%, which increased with increasing amount of synthetic component from P1 to P4 (Figure 2c). The hydrogels crosslinked with MBA presented lower EWC, between 80% and 92%, with the same increasing trend from T1 to T4 due to the amount of the PAA component. The hydrogels Ti (i = 1 - 4) presented intermediary EWC between the control GELMA (T0) and PAA (T0') hydrogels (Figure 2c). Very interestingly, this indicates that the synthetic component, even when crosslinked with MBA, plays the role of a diluting agent for the GELMA macromolecular sequences, inducing increased water affinity of the hybrid hydrogel. On the other hand, augmenting GELMA from T4 to T1 decreased the EWC of the corresponding hydrogels since strong crosslinking hinders both the mobility and the relaxation of the macromolecular chains. Such behaviour proves the crosslinking efficiency of GELMA macromonomer.

Kinetics and mechanism. For some biomedical applications, not only the swelling extent is important, but also the swelling rate, since this can provide information on how fast a defect can be filled or how fast a drug can be absorbed or released [26]. In this respect, a rapidly decreasing swelling rate was observed as a function of time for all the studied materials (Figure 2a and figure 2c). This represents a typical behavior of hydrogels and is due to a decrease in the mobility of the solvent molecules as a result of the water saturation of the network. This is more visible for the series P1-P4. For example, the hydrogels in which GELMA are the dominant component (P1, P2) reached the maximum swelling degree (MSD) in less than 30 hours, unlike the hydrogels in which PAA is the predominant component (P3, P4) reaching the MSD in 50 hours. Thus, increasing the PAA content leads not only to a higher swelling, but it also increases the time necessary to reach the maximum swelling degree. Furthermore, the swelling kinetics were computed using the equation (5). The natural logarithm is:

$$ln\, f = ln\, k + n ln\, t \quad (8)$$

The value of the swelling exponent *n* was obtained as the slope of the linear plot, while the intercept gave *ln k*. It has been demonstrated that for cylindrical hydrogels when *n* values are below 0.5, the swelling is diffusion controlled (Fickian diffusion), while *n* values between 0.5 and 1 are representative for relaxation-controlled swelling [6]. Table 2 presents the results characterizing the GELMA-PAA hydrogels studied. The swelling mechanism changes from relaxation-controlled for samples P1 to P4 to diffusion-controlled for the hydrogels T1 to T4. A general decrease of the swelling exponent with increasing PAA content was noticed. This result differs from other studies reporting that augmenting the PAA content was associated with higher n values [6, 28]. Such differences can be explained through the structure of the GELMA-PAA network consisting of covalently combined components, when compared to PAA-fibroin sIPNs [6, 28].

Table 2. Influence of the composition on the water transport mechanism of GELMA-PAA hydrogels.

GELMA-PAA hydrogel	*n*	*k*	*Swelling mechanism*
P1	0.558	0.004692	Relaxation-controlled
P2	0.558	0.00522	
P3	0.5092	0.006014	
P4	0.5039	0.006019	
T1	0.3249	0.000672	Fickian diffusion
T2	0.2744	0.000762	
T3	0.2676	0.000783	
T4	0.2405	0.000898	

These results are extremely interesting emphasizing the effect of the composition over the swelling behaviour, both in terms of balance GELMA-PAA and also in terms of crosslinking density. Overall, it can be concluded that GELMA-PAA bicomponent hydrogels are characterized by a remarkably high control over the swelling mechanism ensured only by the simple variation of the composition in the polymerization mixture.

Morphology examination by scanning electron microscopy

Non-porous hydrogels. Scanning electron microscopy (SEM) images of the surfaces of the longitudinal sections and cross-sections of the hydrogels revealed that the two types of structural units, AA and GELMA form a continuous phase in all the bicomponent polymer hybrids studied. No phase separation was noticed even at magnifications as high as 100,000 x (examples are shown in figure 3). At low magnification (2,000 x), the presence of blade traces was noticed, more visible on the samples containing high GELMA content. This suggests the hydrogels had different elasticity at their maximum swelling degree. Hydrogel T0 (figure 3a1) consists exclusively of crosslinked GELMA and it seems to be less elastic when compared to sample T2 (figure 3b1) containing 50/1 "C=C" ratio AA/GELMA and sample T4 (figure 3c1) containing 20 times more AA (1000/1 AA/GELMA). This observation was confirmed by other methods and will be further discussed.

Journal Name RSCPublishing

ARTICLE

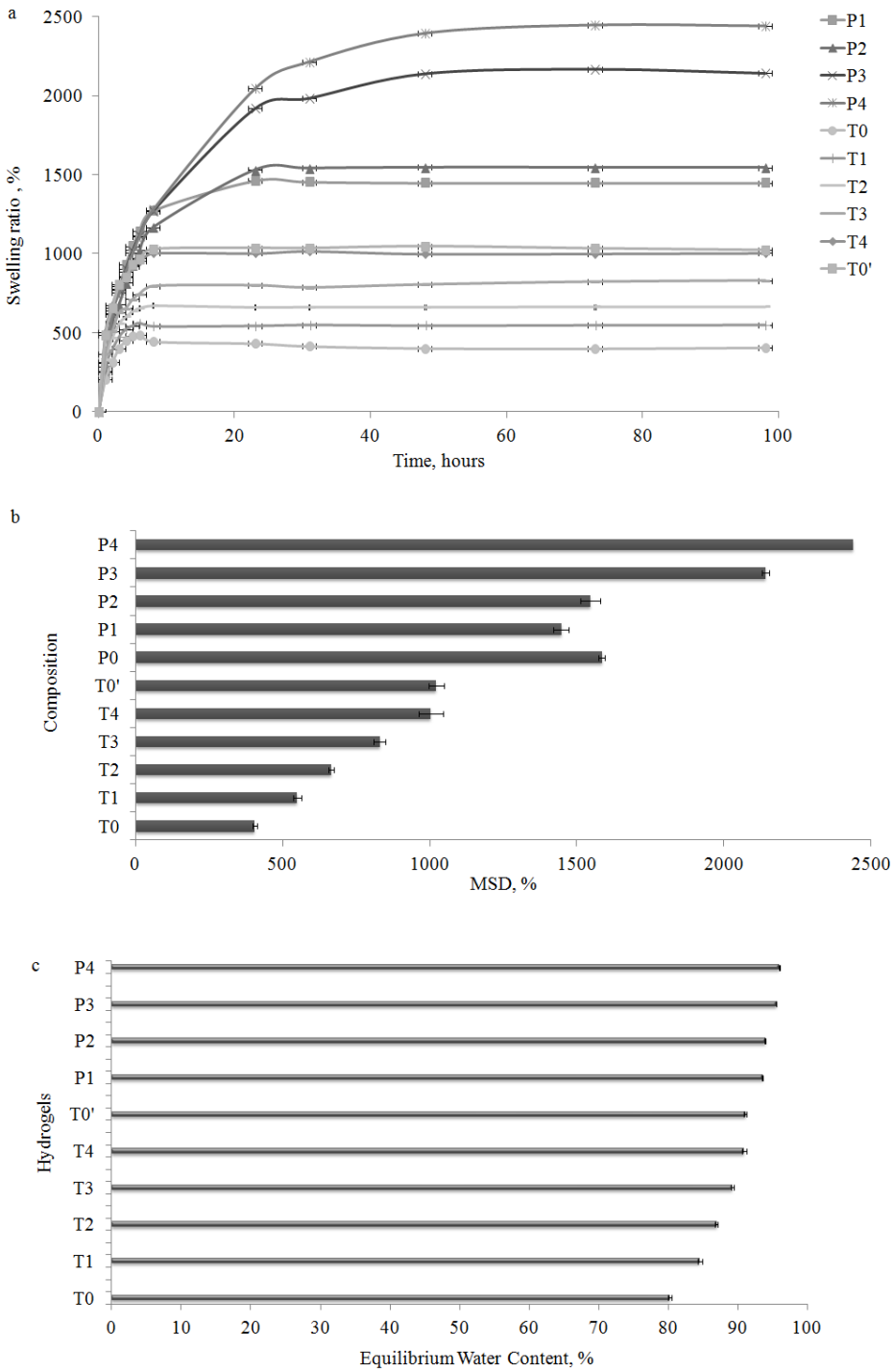

Fig. 2. Swelling behaviour of GELMA-PAA hydrogels: a - swelling ratio as a function of time; b - maximum swelling degree as a function of composition; c - equilibrium water content as a function of composition. (n = 3, mean ± standard deviation)

Journal Name RSCPublishing

ARTICLE

Porous hydrogels. The micrographs of the porous scaffolds T1-T4 obtained through freeze-drying indicated that open and interconnected pores were observed throughout the materials (figure 4). The morphology of the pores, in terms of size and shape, strongly depended on the composition of the hydrogels. Overall, it was noticed that the size of the pores decreased with an increase of AA in the feed ratio, while the total solid content was constant. For example, T1 contains the highest GELMA content and it is associated with relatively spherical large pores, with average dimensions of around 450 µm separated by walls of around 20 µm thickness. T2 presents similar morphology of the pores. A further increase of the amount of synthetic component in T3 and T4 leads to a significant modification of the pore size. Interestingly, two families of pore sizes were visible, one with dimensions around 300 - 400 µm, and one with smaller pores with diameters of approximately 60 µm. Since GELMA-PAA materials were rendered porous after freezing of the maximum water-swollen scaffolds, it may be assumed that such morphological variations are due to compositional differences. Furthermore, it may be presumed that the smaller pores from T3 and T4 correspond to areas where PAA accumulates being the dominant component with respect to GELMA (see table 1). Other studies also reported a decrease in pores size associated with higher PAA amount in bicomponent polymer systems such as silk fibroin-PAA sIPN [6, 28]. Furthermore, porous structures were identified on the surface of the separation walls of samples T4, as shown in Figure 5.

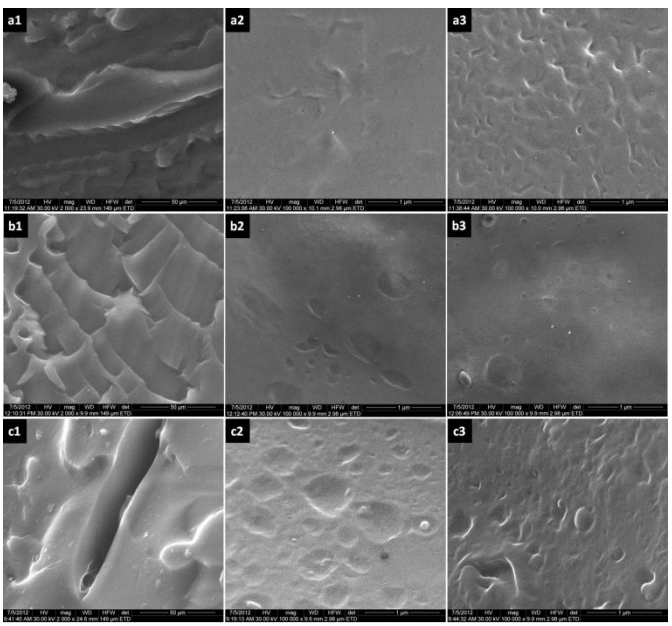

Fig. 3: SEM micrographs representative for the surfaces of a- T0, b - T2, c - T4; 1 - cross-sections at a magnification of 2,000 (scalebar represents 50 µm), 2 - cross-sections at a magnification of 100,000 (scalebar represents 1 µm), and 3 - longitudinal sections at a magnification of 100,000 (scalebar represents 1 µm).

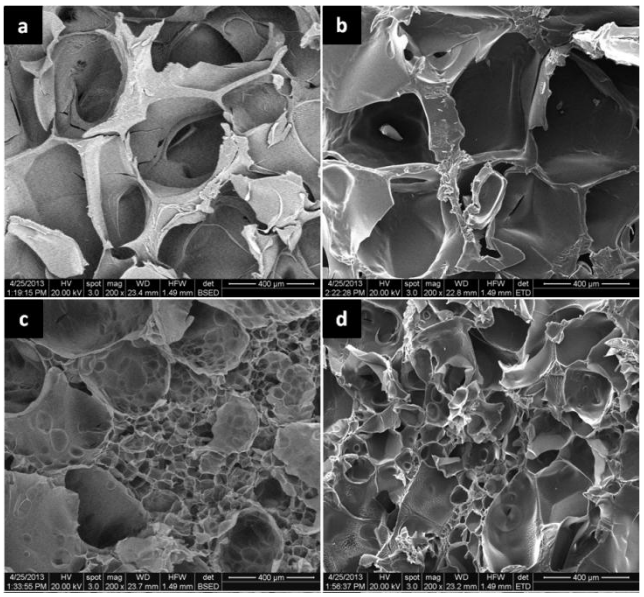

Fig. 4: SEM micrographs representative for cross-sections of the porous scaffolds: a - T1, b - T2, c - T3; d - T4, respectively at a magnification of 200. Scalebar represents 400 µm.

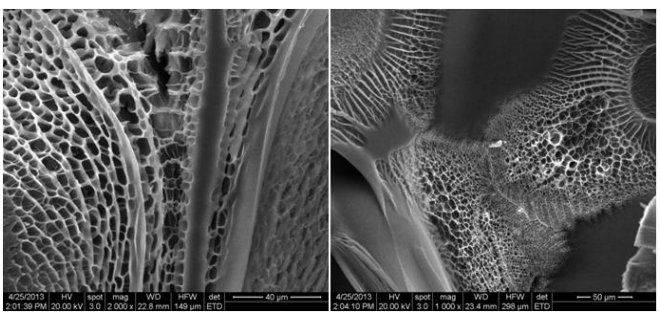

Fig. 5: SEM micrographs representative for porous structures on the surface of the separation walls in T4.

In vitro degradation

pH – dependent stability study in aqueous solutions. To investigate the stability of the hydrogels in different physiological conditions, GELMA-PAA samples were incubated in buffer solutions with pH values of 3, 7.4 and 11, for 0, 48, 72, 96 and 168 hours, respectively. The swelling ratios were computed using equation (3). The bicomponent hydrogels presented stability when immersed for 48, 72, 96 and 168 hours in buffers with pH values of 3 and 7.4, respectively (Figure 6a). The equilibrium values of the bicomponent materials were not modified when changing the pH from 3 to 7.4. Similar results were also reported by other groups [6]. Increasing PAA content in the hydrogels increased the affinity for the incubation media, similarly to the swelling behaviour in water. Moreover, all compositions reached equilibrium swelling after 48

hours, as opposed to the samples incubated in buffer solution with pH 11 for which the swelling continued even after that period of time (see figure 6a). Interestingly, swelling or even fragmentation of the hydrogels (T0 after 72 hours) was noticed at pH 11, as indicated in figure 6a. This fact can be explained through the partial hydrolysis of the PAA component in alkaline medium. The PAA component of the hydrogels is non-ionic but it easily undergoes alkaline hydrolysis leading to ionic sequences with randomly distributed polar carboxyl groups. The composition of the hydrogels influences the intensity of the repulsion forces between ionized carboxylic groups leading to extended and uncoiled polymer chains in the incubation medium. It is known that in such a situation the effective volume of the macromolecular chains increases, leading to larger hydrodynamic interactions with water molecules [31]. We assume that such an effect is proportional to the amount of PAA component in the bicomponent hydrogels, explaining the experimental observation that the sample P4 with the highest PAA content becomes a viscous gel impossible to become weighed after 168 hours. On the other hand, the GELMA component is also responsible for the loss of stability of the hydrogels at pH 11. This presumption was based on the fragmentation of the GELMA hydrogel (T0 in figure 6a) after only 72 hours at pH 11, when compared to the bicomponent compositions. It was presumed that repulsions between carboxylic acid groups from GELMA occur at this pH value. Therefore, while PAA sequences uncoil, carboxylic acid groups from GELMA increase the repulsion intensity enhancing the swelling and the subsequent fragmentation. Since a GELMA monocomponent hydrogel lost its stability and integrity after 72 hours at pH 11, a protein quantitative detection was performed in the incubation medium. Accordingly, the BCA assay was used and the mass loss was estimated using equation (6). The experiment confirmed a degradation of the hydrogel network as shown in figure 6b. All the hydrogels degraded, the mass loss decreasing with an increasing amount of synthetic component. PAA has a dual role at pH 11: (i) on the one hand it increases the overall stability of the bicomponent materials when compared to GELMA monocomponent hydrogels and, (ii) on the other hand, through fast swelling and partial hydrolysis, it facilitates the penetration of the incubation medium to the GELMA sequences. In conclusion, the stability of GELMA-PAA hydrogels is also a remarkably tunable property that can be simply controlled through the composition of the polymerization mixture.

Enzymatic degradation. The enzymatic degradation was investigated and the results are plotted in figure 6c. As anticipated, increasing PAA enhances the stability of the bicomponent hydrogels to enzymatic degradation, while GELMA hydrogels (T0 in figure 6c) totally degrade after only 7 hours. On the other hand, covalently linked GELMA sequences add enzymatic degradability to the bicomponent scaffolds based on PAA. Composition changes may be extremely useful when aiming at controlled biodegradation, in addition to other advantages of these two components.

Mechanical properties

The control of the mechanical properties represents a main concern when designing new polymer scaffolds for potential *in vivo* uses. All mechanical tests were performed using fully hydrated hydrogel samples. The compressive modulus was estimated at 5% deformation and the results are presented in figure 7. Two main compositional factors are influencing the compressive behaviour. Increasing the PAA amount while keeping constant the total solid content in the polymerization mixture decreased the compressive modulus and accordingly, increased the elasticity of the bicomponent hydrogels. On the other hand, additional crosslinking with MBA under the described synthesis procedure generates stronger gels, with higher compressive modulus and lower elasticity when compared to the hydrogels P1-P4. These data are in perfect agreement with the swelling behaviour of GELMA-PAA in water, the elasticity of the materials being justified by the corresponding equilibrium values. Furthermore, when compared to the control hydrogels GELMA (T0, compression modulus 223.76 ± 33.06) and PAA (T0', compression modulus 76.38 ± 12.85), the bicomponent hydrogels present remarkably tunable elasticity. Accordingly, if more elastic materials than T0 are needed, increasing PAA is the solution. The hydrogel T1, rich in GELMA component, already presented a decrease of the compressive modulus from 223.76 ± 33.06 kPa for T0 to 110.72 ± 13.02 kPa. Further augmenting the PAA content enhances the elasticity. Our data differ again from results obtained for sIPNs such as fibroin-PAA, characterised by a decrease of the elasticity with increasing PAA content [6, 28]. Such difference is assigned to the difference in the synthesis procedure: GELMA-PAA hydrogels are obtained with increasing PAA content keeping the total solid content of the polymerization mixture constant, while the sIPNs are obtained only by modifying the ratios fibroin-PAA. The two approaches strongly influenced the evolution of the network density in each hydrogel series as already described for swelling.

Journal Name RSCPublishing

ARTICLE

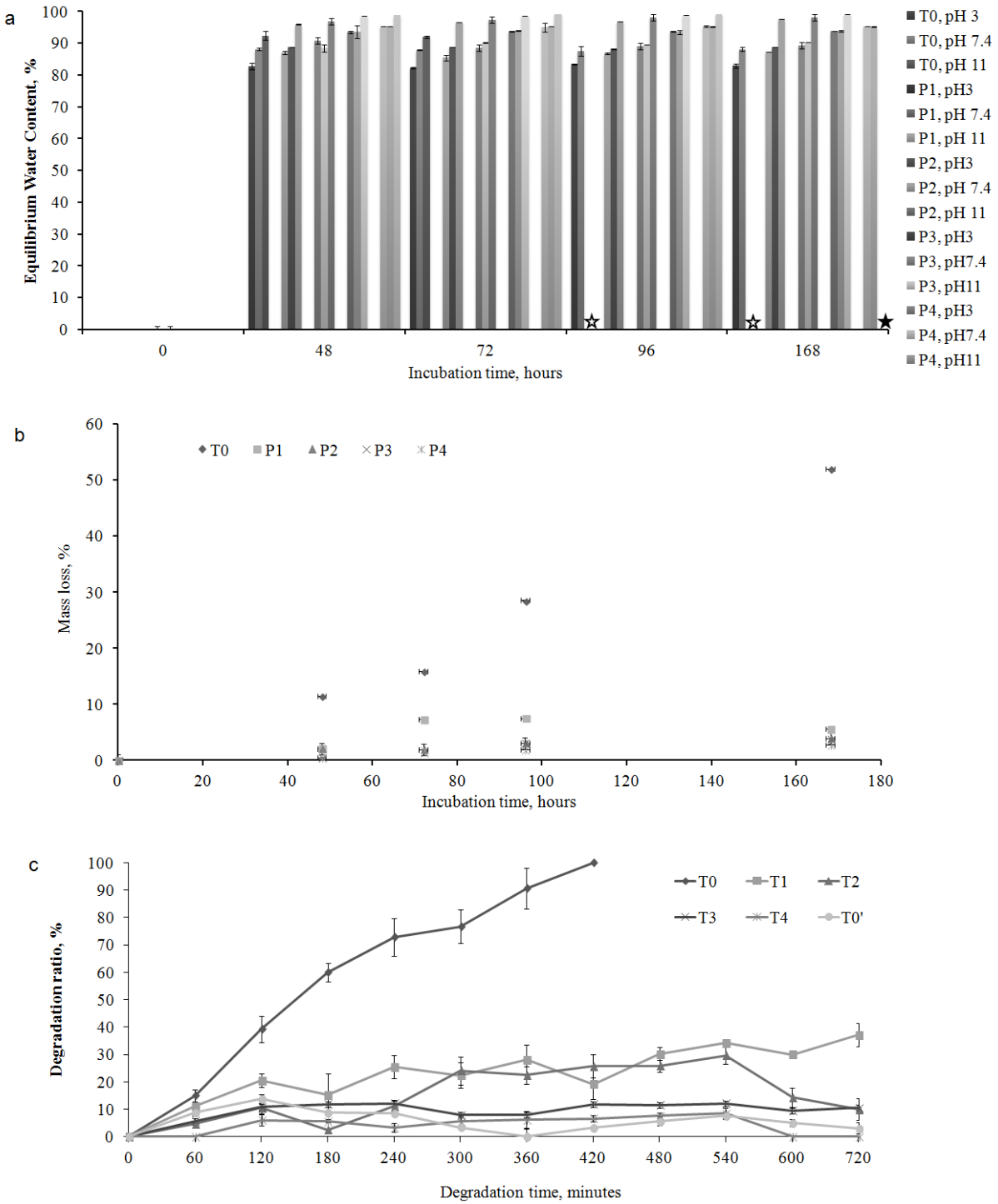

Fig. 6: Hydrogels' stability *in vitro*: a) EWC values at predetermined time intervals after incubation in buffer solutions with pH 3, 7.4, and 11, respectively; white star - T0 lost its integrity through fragmentation; black star - P4 became a viscous gel, impossible to weigh. b) Mass loss (%) as estimated from BCA assay in buffer solution pH 11; c) Degradation ratio (%) after collagenase treatment.

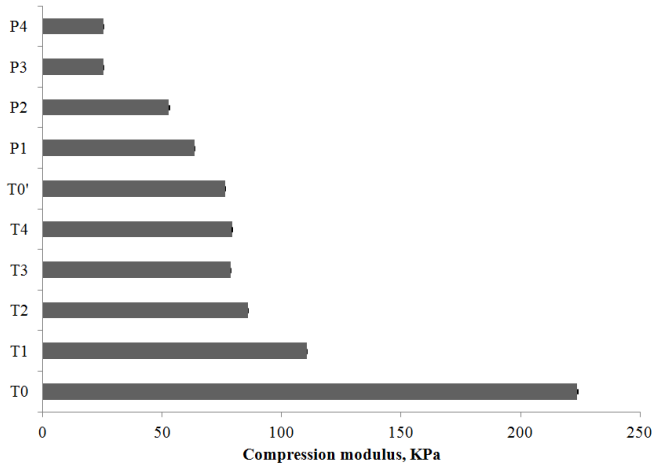

Figure 7. Compressive modulus as computed at 5% deformation, under uniaxial compression of fully hydrated hydrogels. (n = 3, mean ± standard deviation)

The influence of the composition of GELMA-PAA hydrogels was established. Drug release from hydrogel scaffolds is influenced by factors such as the density of the network and the equilibrium water content. It is well known that hydrogels with higher swelling are expected to release higher amounts of solutes when compared to hydrogels with lower swelling. Our study on the release of sodium nafcillin supported the anticipated behaviour as shown in Figure 8. More specifically, the maximum drug release value from the monocomponent hydrogel PAA (T0' in Figure 8) after 10 hours was 91.05 ± 3.47 % from the loaded antibiotic. The other monocomponent hydrogel, GELMA (T0 in Figure 8), had a lower release capacity in the same time interval, releasing only 47.44 ± 1.61 % of the immobilized drug. The bicomponent GELMA-PAA hydrogels presented an increasing drug release capacity from T1 to T4, with intermediary values between the two control samples GELMA (T0) and PAA (T0'). These data were consistent with the above-described water affinity of the bicomponent hydrogels and suggest a variable drug release capacity that can be simply modulated through the composition of the polymerization mixture.

Antibiotic release

The potential of bicomponent hydrogels for drug delivery was preliminary assessed using sodium nafcillin as model antibiotic.

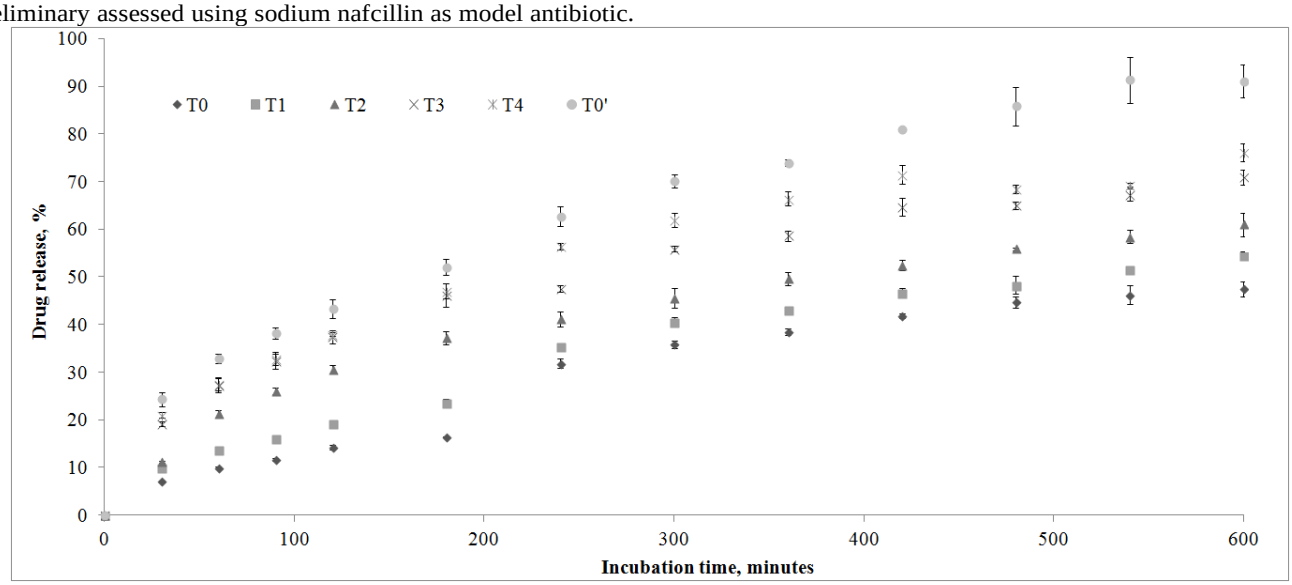

Figure 8. Influence of the composition of bicomponent GELMA-PAA hydrogels on the *in vitro* release of sodium nafcillin, in time. (n = 3, mean ± standard deviation)

Cell adhesion tests

MTT assay. PAA is recognized as a biocompatible polymer not promoting cell adhesion. To evaluate the biocompatibility and cell adhesion promoting properties of GELMA-PAA bicomponent hydrogels, L929 murine fibroblasts were seeded on disks punched from 1 mm thick hydrogel foils and allowed to proliferate for 24 hours and 7 days before being tested (Figure 9a and Figure 9b, respectively). Three bicomponent hydrogels were selected for this study, with decreasing GELMA content from T1 to T3. To allow separate measurements of viability and adhesion, cells that were either weakly adherent or growing in suspension were removed by pipetting and assayed separately.

Culturing the cells on simple PAA hydrogel (T0') for both 1 and 7 days, did not strongly impact overall viability and proliferation (~ 0.9 cell ratio in comparison to tissue culture plastic). However, it did substantially hinder adhesion, as the majority of cells were easily removed by gentle pipetting (adherent cell fraction 0.14+-0.02 at 24 hours and 0.29+-0.02 at seven days). Conversely, cells grown on the GELMA hydrogel (T0) showed an increased adherence at both time-points with 0.35 ± 0.01 and 0.64 ± 0.02 adherent cell ratios at one and seven days, respectively.

Incorporation of GELMA in the bicomponent hydrogels led to an approximate two-fold increase in the adherent cell fraction at 24 hours as compared to PAA, thus showing an improved biocompatibility of these compositions. Moreover, cellular adhesion is ratio dependent as on all of the 3 tested compositions, there was a slight increase in the adherent cell fraction as compared to PAA negative control, reaching statistical significance for T3 at 24 hours, and for T2 and T3 by 7 days.

Fluorescent microscopy. Adherent cells cultured for 7 days on different hydrogel compositions were analyzed by fluorescence microscopy with acridine orange (AO) and propidium iodide (PI) staining. This allowed evaluation of the cell morphology and the visualization of late apoptotic and necrotic cells (PI permeable).
On simple PAA (sample T0' in Figure 9c), cells grew as large, floating multicellular clumps / spheroids (data not shown), characteristic for L929 proliferation on substrates with reduced adhesion promoting properties where cell-to-cell adhesion is dominant [32, 33].

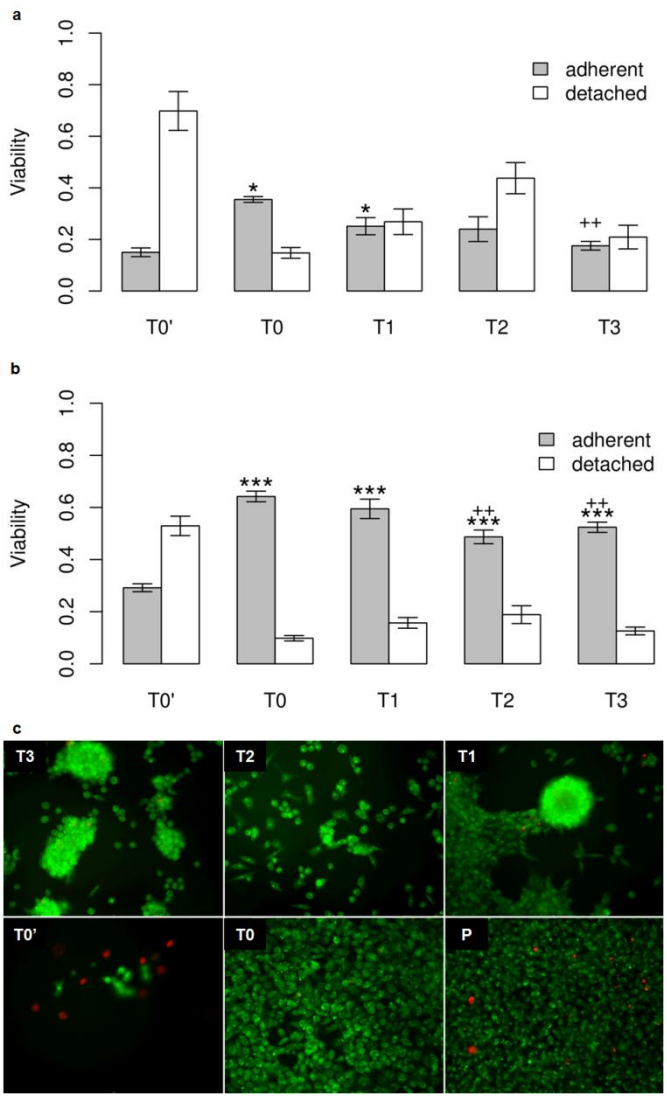

Figure 9. a - Viability as measured by MTT assay of cells cultured for 24 hours on different hydrogels. (Graph represents mean ± SEM, n=6 wells/group). Values are normalized to cells grown on tissue culture plastic. * $p < 0.05$ as compared to T0', ++ $p < 0.01$ as compared to T0. b - Viability as measured by MTT assay of cells cultured for 7 days on different hydrogels. (Graph represents mean ± SEM, n=6 wells/group). Values are normalized to cells grown on tissue culture plastic. *** $p < 0.001$ as compared to T0', ++ $p < 0.01$ as compared to T0. c - Fluorescence microscopy of cells seeded on different substrates. L929 cells were cultured for 7 days on different hydrogels and double stained with AO / PI. P – control cells on tissue culture plastic.

The few cells that remained on the PAA surface were mainly found close to disk borders (where adhesion is probably favoured by surface imperfections resulting from mechanical processing) and most of them showed signs of necrosis (Figure 9c, T0, cells with orange nuclei). On T0 hydrogels, the cells grew in monolayers covering most of the surface while maintaining their normal morphology. Only a very small fraction was PI permeable (Figure 9c, T0). Interestingly, identical cultures on tissue culture plastic were already overgrown, and a large number of cells had already started to become apoptotic (condensed chromatin that stained either bright green or orange).
On hydrogels with variable GELMA-PAA ratios, the cells grew as mixed cultures, where both single cells and cell clumps were observed adhering to the substrate (Figure 9c, T1, T2, T3). Interestingly, although adherent cell numbers, as measured by the MTT assay, only marginally differed between T1, T2 and T3, microscopic examination of the cultures revealed changes in cell growth characteristics that were consistent across multiple fields and replicate wells. Thus, on T3 cultures grew mostly as large adherent clusters, comprising tens of cells with a roughly round shape (Figure 9c, T3) and limited surface coverage. On T2 more cells with spindle shaped / polygonal morphology that were evenly distributed across the observation field were noticed, as well as a reduction in both the number as well as the cellularity of clusters. T1 hydrogels showed large patches of adherent, polygonal cells that covered large areas, but were intermittently scattered across the surface. In addition, occasional spheroids, adherent to cell patches were observable on T1. Such behaviour confirmed the positive role of GELMA component on the cell adherence potential of GELMA-PAA bicomponent hydrogels. This is consistent with the results we recently reported for GELMA-PHEMA hydrogels prepared using a similar one-step polymerization, the protein sequences significantly improving the biocompatibility of the resulting bicomponent hydrogels [4]. Furthermore, the influence of GELMA was similar to results by Jaiswal et al [33] who reported on the beneficial effect of gelatin to impart ECM mimetic microenvironment when intercalated into the three-dimensional network of PAA crosslinked with polycaprolactone diacrylate. Furthermore, our work indicated that the composition of GELMA-PAA bicomponent hydrogels can be modified to provide specific cell-related interactions.

4. Conclusion

Methacrylamide-modified gelatin and acrylamide were successfully covalently bound to obtain inexpensive bicomponent hydrogels with programmable properties through an easy process consisting in a one-pot polymerization reaction. The developed chemical approach combines the two components in a complex natural-synthetic network using an effortless one-step procedure. This represents an important

advantage when compared to the synthesis of gelatin-PAA interpenetrating polymer networks through a two-step procedure usually involving the polymerization of acrylamide followed by the crosslinking of gelatin. The most desirable features of our approach include (1) the simplicity of the network-forming polymerization of C=C double bonds from GELMA and acrylamide leading to complex networks with natural and synthetic sequences and (2) the remarkable versatility of the material properties simply by rational modification of the polymerization mixture. The two macromolecular sequences formed complex natural-synthetic hybrid networks through hydrocarbon chains generated by the polymerization of C=C bonds. The properties of the bicomponent hydrogels were investigated, namely water affinity, stability at different pH values, enzymatic biodegradation, mechanical properties, drug release potential and cellular response. The performed composition-properties correlation allows further control over the material characteristics. Accordingly, it was demonstrated that the addition of PAA sequences into GELMA improved the water affinity, elasticity and capacity to generate porous scaffolds or to release drugs. On the other hand, the presence of GELMA sequences into PAA improved the cellular response of the bicomponent hydrogels, thus broadening the range of potential applications of this new class of materials. Overall, in addition to the described advantages of the new class of GELMA-PAA hydrogels, this study emphasizes the network-forming polymerization of GELMA with synthetic monomers as an appealing chemical strategy to develop new multicomponent natural-synthetic hydrogels with rationally controlled performances for various biomedical applications.

Acknowledgements

The Romanian authors would like to thank the National Research Council (Unitatea Executiva pentru Finantarea Invatamantului Superior, a Cercetarii, Dezvoltarii si Inovarii (UEFISCDI) – Romania) for the Grant no: PNII 183/2012, Programme: Joint Applied Research Projects, SmartBIMBBone, having proved financial support for this work. Dr. Eugeniu Vasile is kindly acknowledged for SEM analyses. The Belgian authors would like to acknowledge the Research Foundation – Flanders (FWO-Vlaanderen), the BOF (Bijzonder Onderzoeksfonds – UGent, Belgium) and the UGent Multidisciplinary Research Partnership Nano- and biophotonics (2010–2014) for financial support.

Notes and references

1. S. Van Vlierberghe, P. Dubruel and E. Schacht, *Biomacromolecules*, 2011, **12**, 1387-1408.
2. E. R. Aurand, K. J. Lampe and K. B. Bjugstad, *Neuroscience Research*, 2012, **72**, 199-213.
3. S. Bubenikova, I.-C. Stancu, L. Kalinovska, E. Schacht, E. Lippens, H. Declercq, M. Cornelissen, M. Santin, M. Amblard and J. Martinez, *Carbohydrate Polymers*, 2012, **88**, 1239-1250.
4. D.-M. Dragusin, S. Van Vlierberghe, P. Dubruel, M. Dierick, L. Van Hoorebeke, H. A. Declercq, M. M. Cornelissen and I.-C. Stancu, *Soft Matter*, 2012, **8**, 9589-9602.
5. B. B. Mandal, B. Ghosh and S. C. Kundu, *International Journal of Biological Macromolecules*, 2011, **49**, 125-133.
6. B. B. Mandal, S. Kapoor and S. C. Kundu, *Biomaterials*, 2009, **30**, 2826-2836.
7. B. B. Mandal, J. K. Mann and S. C. Kundu, *European Journal of Pharmaceutical Sciences*, 2009, **37**, 160-171.
8. B. B. Mandal, A. S. Priya and S. C. Kundu, *Acta Biomaterialia*, 2009, **5**, 3007-3020.
9. I.-C. Stancu, A. Lungu, D. M. Dragusin, E. Vasile, C. Damian and H. Iovu, *Soft Materials*, 2013, **11**, 384-393.
10. B. Duan, L. A. Hockaday, E. Kapetanovic, K. H. Kang and J. T. Butcher, *Acta Biomaterialia*.
11. H. Aubin, J. W. Nichol, C. B. Hutson, H. Bae, A. L. Sieminski, D. M. Cropek, P. Akhyari and A. Khademhosseini, *Biomaterials*, 2010, **31**, 6941-6951.
12. H. Shin, B. D. Olsen and A. Khademhosseini, *Biomaterials*, 2012, **33**, 3143-3152.
13. M. Santin, S. J. Huang, S. Iannace, L. Ambrosio, L. Nicolais and G. Peluso, *Biomaterials*, 1996, **17**, 1459-1467.
14. J. W. Nichol, S. T. Koshy, H. Bae, C. M. Hwang, S. Yamanlar and A. Khademhosseini, *Biomaterials*, 2010, **31**, 5536-5544.
15. M. Nikkhah, N. Eshak, P. Zorlutuna, N. Annabi, M. Castello, K. Kim, A. Dolatshahi-Pirouz, F. Edalat, H. Bae, Y. Yang and A. Khademhosseini, *Biomaterials*, 2012, **33**, 9009-9018.
16. G. Tan, L. Zhou, C. Ning, Y. Tan, G. Ni, J. Liao, P. Yu and X. Chen, *Applied Surface Science*.
17. W. Xiao, J. He, J. W. Nichol, L. Wang, C. B. Hutson, B. Wang, Y. Du, H. Fan and A. Khademhosseini, *Acta Biomaterialia*, 2011, **7**, 2384-2393.
18. A. Ovsianikov, A. Deiwick, S. Van Vlierberghe, P. Dubruel, L. Möller, G. Dräger and B. Chichkov, *Biomacromolecules*, 2011, **12**, 851-858.
19. H. Bae, A. F. Ahari, H. Shin, J. W. Nichol, C. B. Hutson, M. Masaeli, S.-H. Kim, H. Aubin, S. Yamanlar and A. Khademhosseini, *Soft Matter*, 2011, **7**, 1903-1911.
20. W. Schuurman, P. A. Levett, M. W. Pot, P. R. van Weeren, W. J. A. Dhert, D. W. Hutmacher, F. P. W. Melchels, T. J. Klein and J. Malda, *Macromolecular Bioscience*, 2013, **13**, 551-561.
21. G. Camci-Unal, D. Cuttica, N. Annabi, D. Demarchi and A. Khademhosseini, *Biomacromolecules*, 2013, **14**, 1085-1092.
22. N. Annabi, S. M. Mithieux, P. Zorlutuna, G. Camci-Unal, A. S. Weiss and A. Khademhosseini, *Biomaterials*, 2013, **34**, 5496-5505.
23. Y. Liu and M. B. Chan-Park, *Biomaterials*, 2010, **31**, 1158-1170.
24. J. Han, K. Wang, D. Yang and J. Nie, *International Journal of Biological Macromolecules*, 2009 **44**, 229-235.
25. K. S. Lim, J. Kundu, A. Reeves, L. A. Poole-Warren, S. C. Kundu and P. J. Martens, *Macromolecular Bioscience*, 2012, **12**, 322-332.
26. S. Van Vlierberghe, P. Dubruel, E. Lippens, M. Cornelissen and E. Schacht, *Journal of Biomaterials Science, Polymer Edition*, 2009, **20**, 1417-1438.

27. E. Hoch, C. Schuh, T. Hirth, G. E. M. Tovar and K. Borchers, *Journal of Materials Science: Materials in Medicine*, 2012, **23**, 2607-2617.
28. C. Zaharia, M.-R. Tudora, I.-C. Stancu, B. Galateanu, A. Lungu and C. Cincu, *Materials Science and Engineering: C*, 2012, **32**, 945-952.
29. T.-H. Yang, *Recent Patents on Materials Science*, 2008, **1**, 29-40.
30. I.-C. Stancu, *Reactive and Functional Polymers*, 2010, **70**, 314-324.
31. M. E. Zeynali and A. Rabbii, *Iranian Polymer Journal*, 2002, **11**, 269-275.
32. P. L. Ryan, R. A. Foty, J. Kohn and M. S. Steinberg, *Proceedings of the National Academy of Sciences*, 2001, **98**, 4323-4327.
33. M. Jaiswal, V. Koul, A. K. Dinda, S. Mohanty and K. G. Jain, *J Biomed Mater Res B Appl Biomater*, 2011, **98**, 342-350.

Notes and references

[a] Advanced Polymer Materials Group, University Politehnica of Bucharest, 149 Calea victoriei, Sector 1, 010072, Bucharest, Romania.
[b] "Cantacuzino" National Institute for Research and Development in Microbiology and Immunology, 103 Spl. Independentei, 050096 Bucharest, Romania.
[c] Polymer Chemistry and Biomaterials Group, Ghent University, Krijgslaan 281 (S4), B-9000, Ghent, Belgium.

† main authors. The contribution of Andrada Serafim is the synthesis and characterization of the materials. Catalin Tucureanu performed the biological characterization.

